

Carving-turn and edging angle of skis

T. Sahashi and S. Ichino¹

Department of Electrical Engineering, Daido Institute of Technology, Takiharu Minamiku, Nagoya, Japan

¹Department of Physical Education, Aichi University of Education, Kariya, Aichi, Japan

Abstract

Carving-turn descents were performed with carving skis (shaped skis) and conventional skis. The two types of skis exhibited the following common characteristics during carving turn descents compared to conventional (parallel) turns: the amount of skidding was less and the coefficient of kinetic friction, μ , was smaller than these in a conventional (parallel) turn. On the other hand, the edging angles of both types of skis were wider than those for the parallel turn. Both types of skis exhibited almost the same skidding angle and edging angle. The differences between the two types of skis were as follows: μ of a turn was smaller with carving skis than that with conventional skis. Moreover, the radius of curvature of the sliding track, R , was smaller for carving skis than for conventional skis.

Keywords: carving ski, carving turn, coefficient of kinetic friction, edging angle, side-cut, ski sliding

Introduction

In recent years, carving skis have been widely used and instruction books on their use are in print (Ichino 1999). Carving skis are designed with a wider tip and tail than conventional skis. It is said that routine turns, as well as carving turns, are generally easier with carving skis. To confirm this, Ichino conducted an experimental comparison of carving skis and conventional skis in performing carving turns.

The edging angle, β_O was measured along the ski track on the snow plane formed by carving turns; the angles were 20–40°. β_O of carving turns was almost the same for carving skis and conventional skis. On the other hand, β_O of parallel turns was estimated to be within the range 5–10° based on the measurement of the turning descent by Sahashi & Ichino (1996).

Correspondence address:

Toshio Sahashi, Department of Electrical Engineering, Daido Institute of Technology, Takiharu Minamiku, Nagoya 457-8530, Japan.

Tel.: +81 52 6111 2377, Fax: +81 52 612 5623.

E-mail: sahasi@daido-it.ac.jp

β_O is the angle between the ski bottom and the horizontal plane. In the experiment by Sahashi & Ichino (1996), they verified that $\beta_O = 0^\circ$ meant a straight descent and $\beta_O \neq 0^\circ$ meant a turning descent. On the other hand, the angle between the ski bottom and the inclined plane of a ski slope, generally called the *edging angle*, β , is not a factor in determining the turning direction of a ski.

A parallel turn is a turning descent using a parallel stance and generally contains skidding. A carving turn is characterized by a turning descent without skidding. The skidding angle in the descent shows the angle between the sliding direction and the ski direction. Carving turns were recorded using a video camera and the ski loci derived from sequential photographs were analysed using the method of Sahashi & Ichino (1995). The path of the ski loci proved that the skidding angle in a carving turn was very small at approximately $\pm 1^\circ$. The skidding angles were almost the same for carving skis and conventional skis. The research by Sahashi & Ichino (1998) showed that the skidding angle during a parallel turn is much larger at approximately $\pm 20^\circ$.

The coefficient of kinetic friction, μ , calculated from the loci was smaller during the carving turn with less skidding than the parallel turn with more skidding. The value of μ for a turn was smaller for carving skis than for conventional skis. Ski textbooks by Evans *et al.* (1974) and Maruyama *et al.* (1994) state that skis turn because of their side-cut and that edging shortens the radius of curvature of a side-cut, enabling skis to turn more easily. Thus, we studied the variation in side-cut curvature associated with edging in an effort to prove this assertion.

Experiments

Skis and photographs

The inclination angle α of the ski slope was 10° . We used a video camera to continuously record a test skier passing several markers on the snow slope. The ski locus was derived from these sequential video images at $7.5 \text{ frames s}^{-1}$, using the method of Sahashi & Ichino (1995). Figure 1(a) and (b) show examples of photographs of the carving-turn track on the snow slope. The test skier (Ichino) is an official instructor of the Ski Association of Japan. Skis of length 180 cm were used for this experiment. Throughout this paper, we define a ski sliding mark on the snow slope as a *track* and a ski position derived from photoanalysis as a *locus*. At the time of the sliding experiment, the snow temperature was -6°C (packed powder snow) and wind was almost absent.

Skis and inclination of ski slope

Figure 2(a) shows a schema of a ski slope. The slope has an inclination angle α of 30° . We assume that the skier follows this inclined plane with one ski along the hypothetical dotted curve SOT. The plane KHIJ is an enlarged part of a ski-slide (-track) plane passing through point O. The angle θ between the sliding direction HK at O and the fall line FL is 30° , and at the same time, θ is the tangential angle at point O on the curved track. The ski-slide plane and the inclined plane form an angle β of 20° . The edging angle, β_O , which determines the ski-turning direction, is defined as

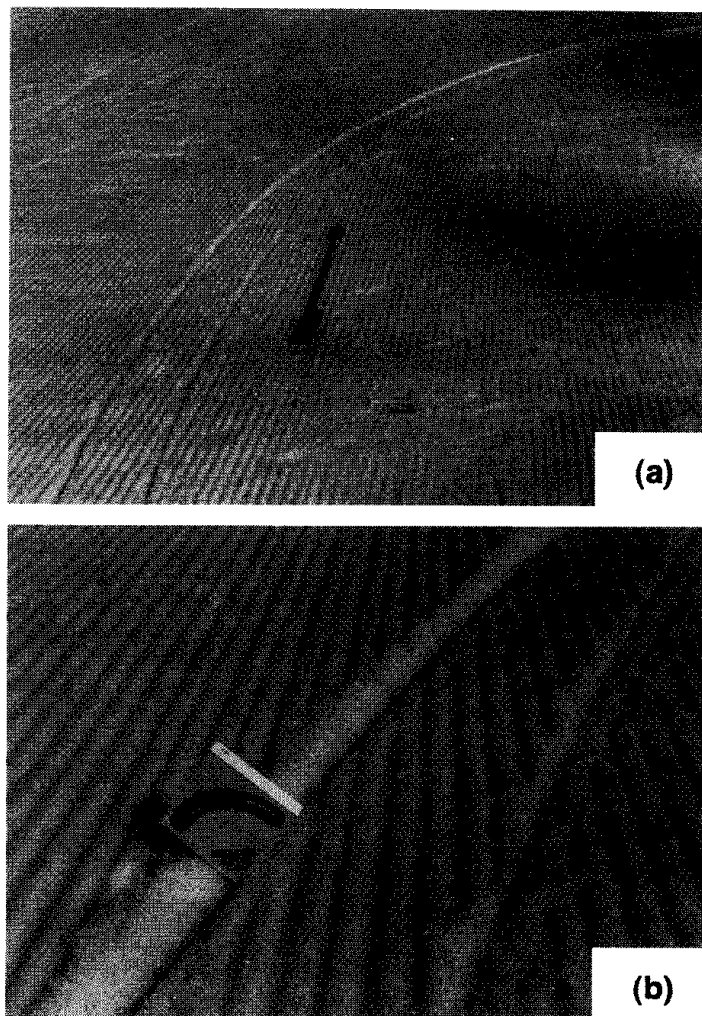


Figure 1 A carving turn using carving skis. (a) Sliding track of a carving turn. (b) Measurement of angle β_O on the sliding plane ($\beta_O = 33^\circ$).

the angle between the horizontal line, NR, and the line MR which is perpendicular to the sliding direction HK on the ski-sliding plane. The edging angle is shown as $\beta_O = 3.9^\circ$ in Fig. 2. The ski continues on an uphill turn after passing point O because the ski-sliding plane slopes in the downward directions, HK and MR. Figure 2(b) shows a section, ABDMR, cut from the ski slope and the ski-slide plane by a plane that is vertical to the sliding direction. The actual sliding plane lies not on the slope, but on the plane carved from the slope by the ski, so that the section should be described as shown in Fig. 2(c). This figure shows that the ski *ac* is tangent to the sliding plane *ab*. The angle $\beta_1 = 16.1^\circ$ is the inclination angle of the slope from the viewpoint of the skier. Let this β_1 be the inclined plane angle. β_1 can be calculated from α ,

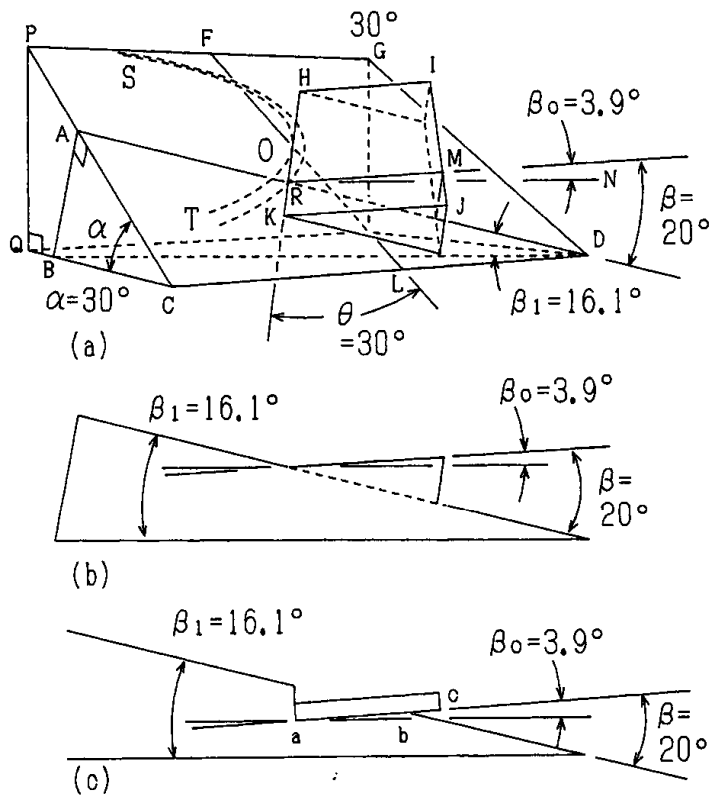


Figure 2 Schema of the ski slope and the ski-sliding plane. (a) The skier skis along SOT on one ski. The sliding plane at point O is enlarged into KHIJ. α is the ski-slope angle and FL is the fall line. θ is the tangential angle, β is the edging angle with respect to the inclined (snow) plane, β_0 is the edging angle with respect to the horizontal plane. (b) The re-described section ABDMR, cut by a plane vertical to the sliding direction from the ski slope and ski sliding plane described in schema (a). (c) The actual state of a sliding ski on the snow plane.

and the tangential angle of sliding track, θ , which is obtained from the loci of the sliding ski (Sahashi & Ichino 1990). The edging angle β can be obtained from the measured value, β_0 and the equation $\beta = \beta_0 + \beta_1$.

Ski angle δ , tangential angle of ski track θ and radius of curvature R

The ski slope with the inclination angle α is described again in Fig. 3(a). FL is the fall line. When FB indicates the ski-sliding direction, the angle between FB and FL is the tangential angle θ .

Let ψ be the apparent-slope angle when the ski slides at an angle of θ . Using $AB = 1$, $AC = FD = b$, $AF = CD = b$, $BC = c$, $BD = d$, $b = \sin \alpha$, $b = \tan \theta$, and $c = \cos \alpha$, the apparent-slope angle

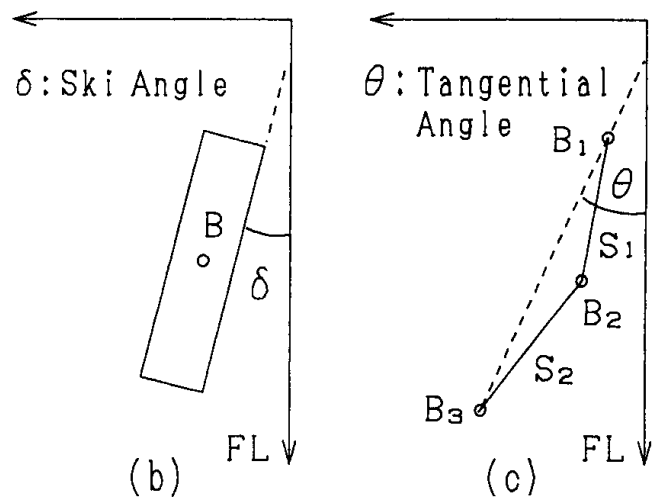
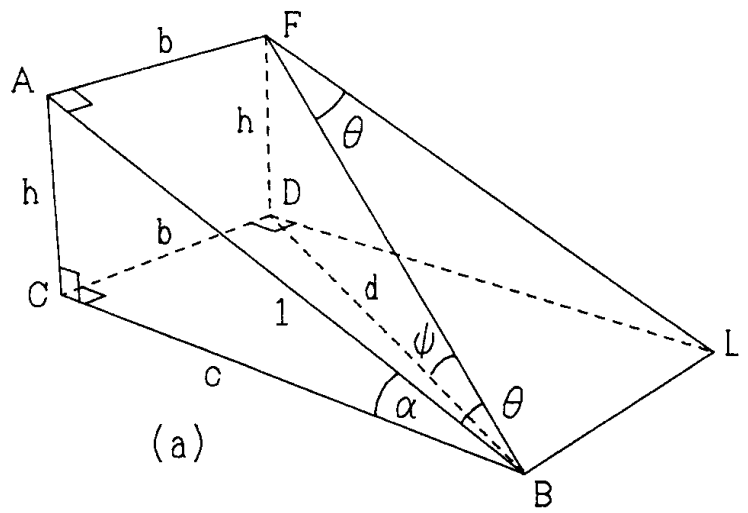


Figure 3 (a) Apparent ski-slope angle ψ . FL is the fall line. ψ is the ski-slope angle in direction θ . (b) Ski angle δ . Point B is the centre of the ski. (c) Tangential angle θ . Point B shifts to B_1 , B_2 , and B_3 as the ski advances. Line B_1B_3 is the tangential line of point B_2 .

ψ can be obtained from the following equation (Sahashi & Ichino 1998):

$$\psi = \tan^{-1}(b/d) = \tan^{-1} \left\{ b / \sqrt{(b^2 + c^2)} \right\}$$

The inclined plane ABLF is described in Fig. 3(b). The angle between FL and the ski is defined as ski angle δ . Let B be the centrepoint of the region of the ski in contact with the snow plane. As the ski slides, the centrepoint B shifts to B_1 , B_2 and then B_3 . Suppose the track passes through points B_1 , B_2 and B_3 and let the tangential angle θ at point B_2 be the angle between FL and the line connecting points B_1 and B_3 . The radius of curvature, R , can also be

obtained from these three points; this is the radius, R , at point B_2 . The difference between δ and θ becomes the skidding angle.

Acceleration of ski: a

In Fig. 3(c), let S_1 and v_1 be the distance and the average velocity between B_1 and B_2 , respectively. Likewise, let S_2 and v_2 be the distance and the average velocity between B_2 and B_3 , respectively. The intervals of time between B_1 and B_2 , and B_2 and B_3 are equal t . Additionally, let g ($= 9.8 \text{ m s}^{-2}$) be defined as the gravitational acceleration and μ as the coefficient of kinetic friction. Then, when B_1, B_2 and B_3 lie on FL, a is the acceleration of the ski at point B_2 and the equation below is obtained by using $S = (S_1 + S_2)/2$, $v_1 = S_1/t$, $v_2 = S_2/t$, $2aS = v_2^2 - v_1^2$:

$$a = g(\sin \alpha - \mu \cos \alpha) = (S_2 - S_1)/t^2.$$

Coefficient of kinetic friction μ in turning descent

When the three points B_1, B_2 and B_3 do not lie on a straight line, the tracks between B_1 and B_2 and between B_2 and B_3 describe curves. Given that the length of these curves can be represented by the straight lines S_1 and S_2 , the acceleration G_C of the ski at point B_2 on the curving track passing through the three points B_1, B_2 and B_3 is formulated, using S_1, S_2, t , and ψ , as

$$G_C = g(\sin \psi - \mu \cos \psi) = (S_2 - S_1)/t^2.$$

G_C is the acceleration of the descent direction of the ski. From the above equation, the coefficient of kinetic friction μ in a turning descent is derived as

$$\mu = (\sin \psi - G_C/g)/\cos \psi.$$

Radius of curvature of side-cut with an edging angle (cylinder approximation)

Figure 4(a) shows a schematic $a'b'c'e'f'g'$ of a ski having a side-cut of radius of curvature R_1 . Figure 4(b) shows a solid model of an obliquely

cut cylinder with radius R_2 , where the section $abck$ is on the horizontal plane. As shown in Fig. 4(b), if a particular β and R_2 are defined, the area of the ski $a'b'c'e'f'g'$ wrapped around the cylinder surface is almost equivalent to the area of the cylinder surface, $abcefg$. Therefore, the sliding ski with the edging angle β on the horizontal plane (snow plane) corresponds to the surface $abcefg$. On the horizontal plane, $\beta = \beta_0$ at all times. To quantitatively analyse Fig. 4(b), we draw the cylinder in side view in Fig. 4(e) and in top view in Fig. 4(c). Figure 4(d) shows an ellipse which appears on the section $abck$. Thus, the side-cut $a'b'c'$ shown in Fig. 4(a) is represented by the solid curved line abc in the ellipse in Fig. 4(d).

In Fig. 4(a), SL is defined as the length of the ski. When the radius of curvature R_1 of the side-cut is given, the halfangle ξ_1 of the arc $a'b'c'$ is obtained from

$$R_1 \sin \xi_1 = SL/2 \tag{1}$$

C'_2 is defined as the width of the shovel of the ski, and is represented by the equation $C'_2 = R_1(1 - \cos \xi_1)$. In Fig. 4(e) and (c), the following equation holds with regard to the radius of the cylinder R_2 and $2\xi_2$. $2\xi_2$ is the central angle corresponding to the arc efg in Fig. 4(c), which angle also corresponds to the length of the ski SL fitted along the surface of the cylinder:

$$SL = 2R_2 \xi_2 \tag{2}$$

C_2 is defined as the width of the shovel of the ski indicated on the cylinder surface and is represented by the equation $C_2 = R_2(1 - \cos \xi_2)/\tan \beta$, where $X_2 = R_2(1 - \cos \xi_2)$ and $X_2/C_2 = \tan \beta$. When β satisfies the condition that the width C'_2 , the shovel of the ski, and the width C_2 , the shovel on the cylinder surface, are equal,

$$C'_2 = R_1(1 - \cos \xi_1) = R_2(1 - \cos \xi_2)/\tan \beta \tag{3}$$

holds. From the above equations, R_2 is obtained, if the values of R_1, SL and β are given. Then, from equations $X_4 = R_2 \cos \xi_2$, $X_4/X_3 = R_2/A = \sin \beta$ and $Y_3/R_2 = \sin \xi_2$, the following expressions are obtained:

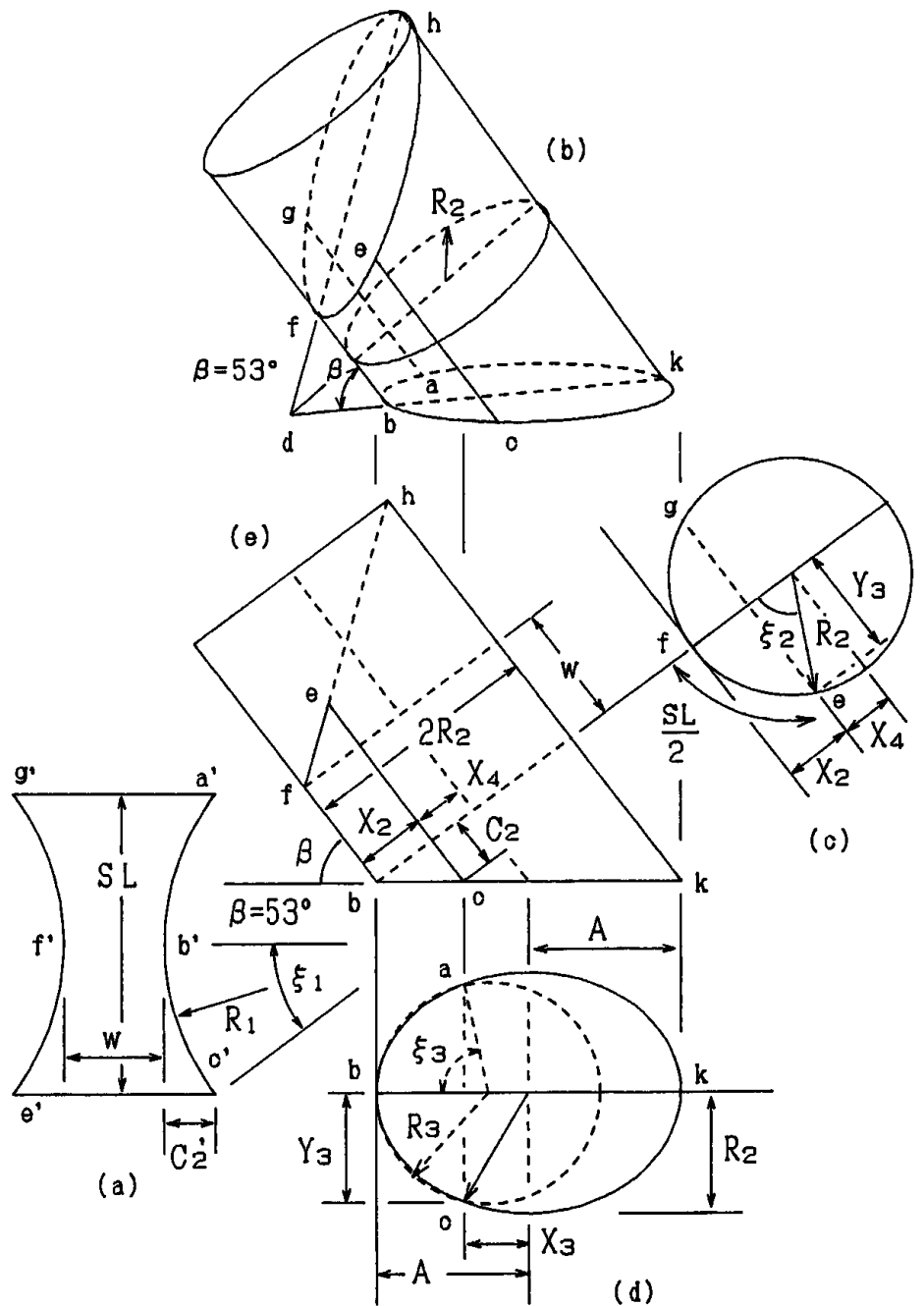


Figure 4 Schema of a ski at an edging angle. (a) A ski shaped like a reel. (b) A ski fitted along the cylinder's surface. (c) Circle of a vertical section of the cylinder. (d) Ellipse of an oblique section of the cylinder. (e) A side view of the cylinder (b).

$$A - X_3 = (R_2 - X_4) / \sin \beta \quad (4)$$

$$Y_3 = R_2 \sin \xi_2 \quad (5)$$

$R_2 = 0.93 \text{ m}$, $R_3 = 0.77 \text{ m}$, $\xi_1 = 36^\circ$, $\xi_2 = 49^\circ$ and $\xi_3 = 60^\circ$.

In Fig. 4(d), suppose that the curved line passing through the three points $(A - X_3, Y_3)$, $(0,0)$ and $(A - X_3, Y_3)$ on the ellipse is roughly equal to the circle of radius R_3 passing through the same three points. Then, the radius R_3 of the circle can be obtained from R_1, SL and β . The ξ_3 , defined as half the central angle corresponding to the arc abc , is obtained from $R_1 \xi_1 = R_3 \xi_3$. Figure 4 is described using $SL = 1.6 \text{ m}$, $\beta = 53^\circ$, $R_1 = 1.28 \text{ m}$,

Results

Carving turn using carving skis

Figure 5(a) shows the locus of a carving turn using carving skis. In this figure, \downarrow denotes the direction of the fall line FL. The vertical axis indicates the distance along the fall line and ski numbers. Since the loci of the skis indicated in Fig. 5(a)

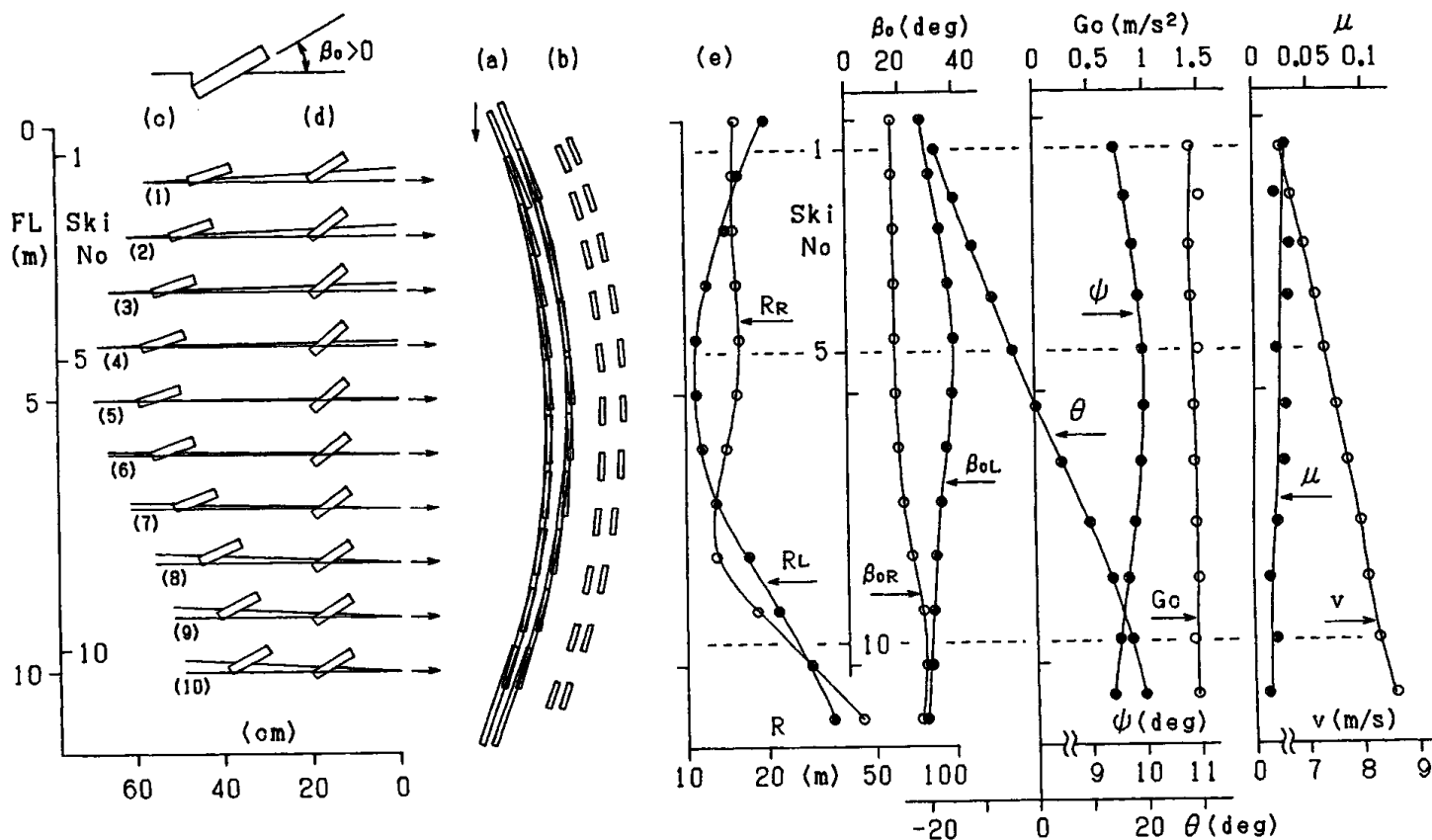


Figure 5 Analysis of the carving turn. (a) Loci of the carving turn using carving ski. (b) Loci of the ski shortened to 50 cm in length. (c) and (d) Edging angle β_0 and inclined plane angle β_1 . (e) R is the radius of curvature of the path of ski loci. β_0 is edging angle, θ is tangential angle, ψ is apparent ski-slope angle, G_C is acceleration of the ski, v is the velocity, and μ is coefficient of kinetic friction.

indistinguishably overlap each other, they are shown at 1 m on the left, shortened to 50 cm in Fig. 5(b). Figure 5(c) and (d) illustrates the edging sequence viewed from the sliding direction of the skis, as well as from the front of the skis, similar to Fig. 2(c). The right ski is indicated in Fig. 5(c) and the left ski is shown in Fig. 5(d). The direction is the one of the tangential angle θ . Figure 5(c) and (d) show the edging angle β_0 , the inclined plane angle β_1 and the distance between the two skis. Let the width of each ski be 10 cm. In Fig. 5(c) and (d), the region of the bottom of the ski in contact with the snow plane, ab shown in Fig. 2(c), is expressed as an arbitrary width. Edging position (1) shows the state in which the midpoint between the right ski and the left ski is located at the 1 m position on the FL, as indicated by the lateral arrow. Likewise, position (2) shows the state at 2 m on the FL, and so forth. In Fig. 5(e), β_{0R} means β_0 with respect to the right ski, and β_{0L} means β_0 with respect to the left ski. R_R is defined as the radius of curvature of

the locus with respect to the right ski and R_L defines the same parameter for the left ski. θ is the mean value of the tangential angles of the right ski and the left ski. Moreover, Fig. 5(e) indicates the following values viewed from the direction θ : the apparent-slope angle ψ , the acceleration of ski G_C , the coefficient of kinetic friction μ and the velocity v .

Comparison between carving skis and conventional skis

The locus of a carving turn using a conventional ski is shown in Fig. 6(a). β_0 on carving skis, indicated in Fig. 5, is similar to that of conventional skis shown in Fig. 6. The radius of curvature of the locus, R , was 10–20 m on carving skis, which is smaller than that for conventional skis (20–30 m). The acceleration of carving skis, G_C , was greater than that of conventional skis. Carving skis had a smaller μ than conventional skis.